Testing the Kerr spacetime with X-ray reflection spectroscopy

Masoumeh Ghasemi-Nodehi
National Astronomical Observatories, Chinese Academy of Sciences,
Beijing 100101, China
E-mail: ghasemi@nao.cas.cn

Astrophysical black holes are thought to be Kerr solution of general relativity but their Kerr geometry have not yet verified. Iron line is prominent feature in X-ray reflection spectra. Shape of iron line in X-ray reflection spectra of both stellar-mass and super massive black hole candidates are supposed to be strongly affected by spacetime geometry. This method is a powerful technique to prob strong gravity regime and deviations from Kerr spacetime. In this talk, I present iron line of some non-Kerr spacetimes. I also present data simulations of X-ray missions. The purpose is to understand whether X-ray reflection spectroscopy can distinguish these non-Kerr spacetimes from Kerr solution of general relativity.

Keywords: Tests of General Relativity, X-ray Reflection Spectroscopy.

1. Introduction

Final product of gravitational collapse is Kerr spacetime according to Einstein's theory of general relativity. General relativity is strongly constrained by weak field regime experiments. There have been efforts to test strong gravity regime by probing the metric around astrophysical candidates in the recent years [1]. The studies are based on properties of electromagnetic radiation emission of accretion disk. Kerr black holes are only characterized by mass and spin based on multipole moment expansions. Higher multipole moment expansions in a Kerr spacetime are only function of mass and spin. The compact object cannot be the Kerr black hole of general relativity in the case of measurement of independent higher multipole moments such as quadrupole moment by observational data.

Neutron stars have high density and strong gravity. They are fascinating laboratory to study possible deviation from prediction of general relativity, and in general, to study strong gravity regime. Multipole moment expansion can provide accurate approximation of spacetime surrounding a neutron star. Study of higher order multipole moments can reveal properties of neutron stars.

Approximate solution of exterior spacetime of neutron star is presented in reference [2]. The solution is based on Ernst formulation of general relativity up to five multipole moments, mass, angular momentum, mass quadrupole, spin octupole, and hexadecapole. The relation between these hairs and neutron star surrounding spacetime is also introduced in the reference. The hairs only depends on mass, spin, and quadrupole moment.

In present paper, I considered this metric based on Ernst formalism up to five multipole moments to study observational test of the neutron star exterior spacetime and distinguish it from Kerr spacetime. I employ iron line method. The iron line is prominent feature in X-ray reflection spectra. The emission is fluorescent narrow lines from geometrically thin and optically thick accretion disk which produced by absorption of a hard X-ray photon of corona. This emission would be broadened and skewed in the inner region of the accretion disk due to relativistic effect of compact object there. In this paper, first, iron lines are simulated. Then, observational data are simulated and analyzed. The result is as follows. It is hard to constrain parameters of neutron star exterior spacetime using iron line method since both fast rotating and slow rotating case cannot be distinguished from Kerr solution of general relativity. The paper is structured as follows. In section 2, I present the spacetime metric. Section 3 is devoted to iron line method and data simulation and analysis is presented in section 3. Finally, section 4.1 is a short summary and conclusion. Throughout the paper, I employ units in which $G_N = c = 1$ and metric signature is $(-,+,+,+)$.

2. Theoretical Framework

A stationary and axially symmetric spacetime based on Ernst potential formalism to describe spacetime surrounding a neutron star is reported in [2]. The solution contains the first five relativistic multiple moments, the mass, M, angular momentum, J, the mass quadrupole, M_2, spin octupole, S_3, and the mass hexadecapole, M_4. The line element reads

$$ds^2 = -f\left(dt - \omega d\varphi\right)^2 + f^{-1}\left[e^{2\gamma}\left(d\rho^2 + dz^2\right) + \rho^2 d\varphi^2\right], \tag{1}$$

where metric functions f, ω, and γ are given as

$$\begin{aligned}
f(\rho,z) &= 1 - \frac{2M}{\sqrt{\rho^2+z^2}} + \frac{2M^2}{\rho^2+z^2} + \frac{\left(M_2 - M^3\right)\rho^2 - 2\left(M^3 + M_2\right)z^2}{\left(\rho^2+z^2\right)^{5/2}} \\
&\quad + \frac{2z^2\left(-J^2 + M^4 + 2M_2M\right) - 2MM_2\rho^2}{\left(\rho^2+z^2\right)^3} \\
&\quad + \frac{A(\rho,z)}{28\left(\rho^2+z^2\right)^{9/2}} + \frac{B(\rho,z)}{14\left(\rho^2+z^2\right)^5}, \\
\omega(\rho,z) &= -\frac{2J\rho^2}{\left(\rho^2+z^2\right)^{3/2}} - \frac{2JM\rho^2}{\left(\rho^2+z^2\right)^2} + \frac{F(\rho,z)}{\left(\rho^2+z^2\right)^{7/2}} \\
&\quad + \frac{H(\rho,z)}{2\left(\rho^2+z^2\right)^4} + \frac{G(\rho,z)}{4\left(\rho^2+z^2\right)^{11/2}}, \\
\gamma(\rho,z) &= \frac{\rho^2\left(J^2\left(\rho^2 - 8z^2\right) + M\left(M^3 + 3M_2\right)\left(\rho^2 - 4z^2\right)\right)}{4\left(\rho^2+z^2\right)^4} - \frac{M^2\rho^2}{2\left(\rho^2+z^2\right)^2},
\end{aligned}$$

where

$$
\begin{aligned}
A(\rho,z) = {} & \left[8\rho^2 z^2\left(24J^2M + 17M^2M_2 + 21M_4\right) + \rho^4\left(-10J^2M + 7M^5 + 32M_2M^2\right)\right.\\
& \left. - 21M_4 + 8z^4\left(20J^2M - 7M^5 - 22M_2M^2 - 7M_4\right)\right],\\
B(\rho,z) = {} & \left[\rho^4\left(10J^2M^2 + 10M_2M^3 + 21M_4M + 7M_2^2\right) + 4z^4\left(-40J^2M^2 - 14JS_3\right.\right.\\
& \left. + 7M^6 + 30M_2M^3 + 14M_4M + 7M_2^2\right) - 4\rho^2z^2\left(27J^2M^2 - 21JS_3\right.\\
& \left.\left. + 7M^6 + 48M_2M^3 + 42M_4M + 7M_2^2\right)\right],\\
H(\rho,z) = {} & \left[4\rho^2z^2\left(J\left(M_2 - 2M^3\right) - 3MS_3\right) + \rho^4\left(JM_2 + 3MS_3\right)\right]\\
G(\rho,z) = {} & \left[\rho^2\left(J^3\left(-\left(\rho^4 + 8z^4 - 12\rho^2z^2\right)\right) + JM\left(\left(M^3 + 2M_2\right)\rho^4\right.\right.\right.\\
& - 8\left(3M^3 + 2M_2\right)z^4 + 4\left(M^3 + 10M_2\right)\rho^2z^2\big)\\
& \left.\left. + M^2S_3\left(3\rho^4 - 40z^4 + 12\rho^2z^2\right)\right)\right]\\
F(\rho,z) = {} & \left[\rho^4\left(S_3 - JM^2\right) - 4\rho^2z^2\left(JM^2 + S_3\right)\right].
\end{aligned}
$$

The first multipole moments can be expressed as follows to use for neutron star case

$$
\begin{aligned}
M_2 &= -\alpha j^2 M^3,\\
S_3 &= -\beta j^3 M^4,\\
M_4 &= \gamma j^4 M^5,
\end{aligned} \tag{2}
$$

where M is mass and $j = J/M^2$ is spin parameter. The case $\alpha = \beta = \gamma = 1$ presents the Kerr case but these parameters can be large for neutron star case. The relation between α, β, and γ is[3,4]

$$
\begin{aligned}
y_1 &= -0.36 + 1.48\,x^{0.65}\\
y_2 &= -4.749 + 0.27613\,x^{1.5146} + 5.5168\,x^{0.22229},
\end{aligned} \tag{3}
$$

where $x = \sqrt{\alpha}, y_1 = \sqrt[3]{\beta}$, and $y_2 = \sqrt[4]{\gamma}$. Thus, one can determine the neutron star exterior spacetime by mass, spin, and parameter α, ranges from ~ 1.5 for non-rotating case to 8 for cases with maximum value of spin parameter such as 0.5.

3. X-ray Reflection Spectroscopy

Iron line is prominent feature in X-ray reflection spectra of astrophysical black hole candidates. Iron atom absorbs hard X-ray photon of optically thin comptonized corona and emits fluorescence lines. This line is at 6.4 keV for weakly ionized or neutral atom and shifts up to 6.97 keV in the case of ionized H-like iron. This line would be broadened and skewed as the result of presence of strong gravity region and relativistic effects such as Doppler shift, gravitational redshift and light bending in the inner region of the accretion disk. This broad and skewed line provide us powerful tool to test strong gravity regime. This observational feature is determined by background metric, viewing angle, and emissivity profile of the disk. In my simulation, the inner edge of the disk is considered at the ISCO radius and the outer edge is large enough that its impact is small. The emissivity is power-law, $1/r^q$, where q is emissivity index. The assumption is $q = 3$ which corresponds to Newtonian limit at large radii. The code is described in [5,6].

The iron lines for metric 1 with two sets of spin parameter 0.5 and 0.2, and viewing angle 55° are presented in figures 1 and 2. The lines present slight difference with respect to Kerr one for case with spin 0.5 and the impact on the line profile with spin 0.2 is weak and maybe harder to constrain.

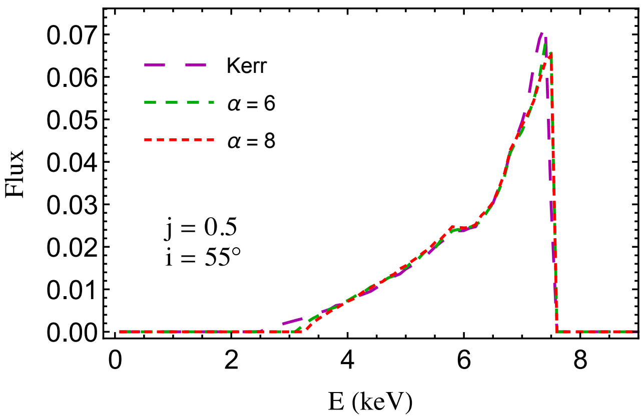

Fig. 1. Spin parameter value is 0.5 and viewing angle is 55°. The parameter values for α are 6 and 8. See text for more details.

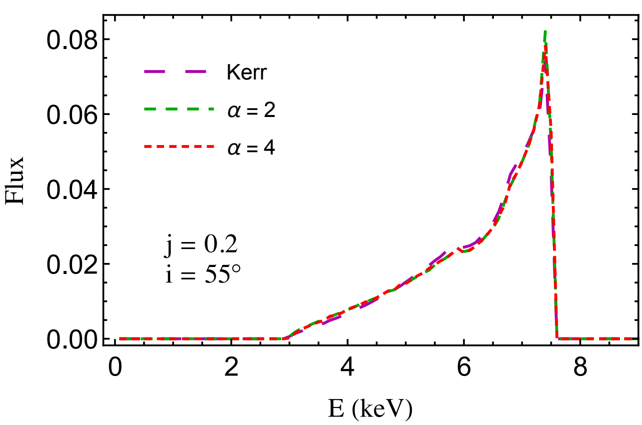

Fig. 2. This figure present the iron lines with spin parameter value 0.2 and viewing angle 55°. The parameter values for α are 2 and 4. See text for more details.

4. Simulating Data and Analysis

In this section, I simulate observed data of a neutron star and analyze them with a Kerr model. This tells us whether the Kerr model fit the data or not. I simulate data with a model consists of power-law and a single iron line of previous section. The considered flux is about 10^{-11} erg/cm^2/s in the range $2-10$ keV for neutron star case. The equivalent width is about 200 eV and photon index of power-law is 2. The simulation is done with *fakeit* command of XSPEC using RMF, ARF, and background file of LAD instrument with large area detector on board of enhanced X-ray Timing and Polarimetry (eXTP) China-Europe mission which is planned to launch before 2025. The LAD instrument has large effective area to provide more counts with less poisson noise. The data fitting is done with a power-law model and a RELINE model (a Kerr iron line). Figure 3 shows data to model ratio of best fit model for neutron star data simulation with spin parameter 0.5 and $\alpha = 8$ in the left panel. Right panel shows the case with spin value 0.2 and $\alpha = 2$. As we see there are slight differences for the case with spin 0.5 and there are not strong effect for spin value 0.2 which means it is hard to be constrained.

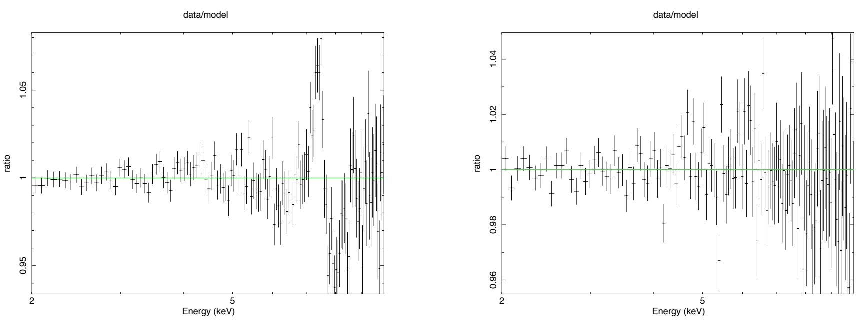

Fig. 3. Left panel: Data-to-model model ratio for simulation with iron line $j = 0.5$, $i = 55°$ and $\alpha = 8$. The reduced χ^2 is 2.1 and there are unresolved features. Right panel: The spin parameter for this figure is 0.5, $i = 55°$ and $\alpha = 2$ for the iron line. The figure shows the data-to-model ratio. The reduced χ^2 is 1.1 and there are no remarkable unresolved features, which makes this case harder constrain.

4.1. *Summary and Conclusion*

A solution of Einstein's field equations using Ernst potential formalism up to five multipole moments is introduced in the reference [2]. This method can accurately describe the exterior spacetime of neutron star. The iron line emitted from medium around neutron star is simulated in the present paper. Two different values of spin parameter 0.5 and 0.2 with different value of α are considered. The impact of iron lines with spin value 0.5 is not very strong and there is no impact on iron lines spin value 0.2. The 100ks observation with LAD-eXTP for neutron star with different sets of parameter value are also presented. If the fit is not good, the neutron star exterior spacetime parameters and the deviations from the Kerr case can be constrained. The fit for higher value of spin parameter 0.5 and $\alpha = 8$ does not seem good. But the impact on iron lines are small and also there are uncertainties. Thus, it might be hard to constrain neutron star solution. The fit for spin value 0.2 and $\alpha = 2$ is good which indicates it is not possible to constrain deviations from Kerr solution.

Acknowledgments

This work is partly supported by the National Key Program for Science and Technology Research and Development (Grant No. 2016YFA0400704), the National Natural Science Foundation of China under grant No. 11690024 and 11390372, and the Strategic Priority Program of the Chinese Academy of Sciences (Grant No. XDB 23040100). I also acknowledge support from the China Postdoctoral Science Foundation, Grant No. 2017LH021.

References

1. J. Schee and Z. Stuchlik, Int. J. Mod. Phys. D **18**, 983 (2009), J. Schee and Z. Stuchlik, Gen. Rel. Grav. **41**, 1795 (2009), T. Harko, Z. Kovacs and F. S. N. Lobo, Phys. Rev. D **79**, 064001 (2009), T. Harko, Z. Kovacs and F. S. N. Lobo, Phys. Rev. D **80**, 044021 (2009), T. Harko, Z. Kovacs and F. S. N. Lobo, Class. Quant. Grav. **27**, 105010 (2010), C. Bambi and N. Yoshida, Phys. Rev. D **82**, 064002 (2010), T. Johannsen and D. Psaltis, Astrophys. J. **726**, 11 (2011), C. Bambi and E. Barausse, Astrophys. J. **731**, 121 (2011), T. Johannsen and D. Psaltis, Astrophys. J. **773**, 57 (2013), C. Bambi, JCAP **1209**, 014 (2012), N. Tsukamoto, Z. Li and C. Bambi, JCAP **1406**, 043 (2014), Z. Li and C. Bambi, Phys. Rev. D **90**, 024071 (2014), C. Bambi, J. Jiang and J. F. Steiner, Class. Quant. Grav. **33**, 064001 (2016), K. Yagi and L. C. Stein, Class. Quant. Grav. **33**, 054001 (2016), T. Johannsen, Class. Quant. Grav. **33**, 124001 (2016), M. Ghasemi-Nodehi and C. Bambi, Phys. Rev. D **94**, 104062 (2016), C. Bambi, Rev. Mod. Phys. **89**, 025001 (2017),
2. G. Pappas, Mon. Not. Roy. Astron. Soc. **466**, no. 4, 4381 (2017) [arXiv:1610.05370 [gr-qc]].
3. G. Pappas and T. A. Apostolatos, Phys. Rev. Lett. **112**, 121101 (2014) [arXiv:1311.5508 [gr-qc]].
4. K. Yagi, K. Kyutoku, G. Pappas, N. Yunes and T. A. Apostolatos, Phys. Rev. D **89**, no. 12, 124013 (2014) [arXiv:1403.6243 [gr-qc]].
5. C. Bambi, Astrophys. J. **761**, 174 (2012) [arXiv:1210.5679 [gr-qc]].
6. C. Bambi, Phys. Rev. D **87**, 023007 (2013) [arXiv:1211.2513 [gr-qc]].